Post-print of: Wiatr M., Jasik P., Kilich T., Sienkiewicz J., Stoll H.: Quasirelativistic potential energy curves and transition dipole moments of NaRb. CHEMICAL PHYSICS. Vol. 500, (2018), p. 80-87. DOI: 10.1016/j.chemphys.2017.10.005

Quasirelativistic potential energy curves and transition dipole moments of NaRb

M. Wiatr [a], P. Jasik [a,*], T. Kilich [a], J.E. Sienkiewicz [a,*], H. Stoll [b]

[a] Department of Theoretical Physics and Quantum Information, Faculty of Applied Physics and Mathematics, Gdansk University of Technology, ul. Gabriela Narutowicza 11/12, 80-233 Gdansk, Poland
[b] Institute for Theoretical Chemistry, University of Stuttgart, Pfaffenwaldring 55, D-70569 Stuttgart, Germany

a b s t r a c t

We report on extensive calculations of quasi-relativistic potential energy curves and, for the first time, transition dipole moments including spin-orbit and scalar-relativistic effects of the NaRb molecule. The calculated curves of the 0^+, 0^-, 1, 2 and 3 molecular states correlate for large internuclear separation with the fourteen lowest atomic energies up to the Na(3s $^2S_{1/2}$) + Rb(7s $^2S_{1/2}$) atomic limit. Several new features of the potential energy curves have been found.

Keywords: Potential energy curves, Spin-orbit effect, MRCI, Spectroscopic parameters Transition dipole moment functions

1. Introduction

The interest in laser cooling and trapping of atoms shifts to polar diatomic molecules since, due to their internal degrees of freedom, they may find broader applications in ultracold chemistry, quantum information and quantum simulations. Particularly, the heteronuclear alkali dimers attract considerable attention as promising candidates for effective photoassociation experiments [1,2] to produce cold and ultracold molecular gas. These require the use of high resolution spectroscopy methods supported by detailed knowledge of interaction between two alkali atoms. Besides lithium as the lightest of alkali atoms, the heavier atoms possess non-negligible energetic fine structure indicating that the spin-orbit coupling has to be taken into account in theoretical calculations. That makes the calculations more complicated but the resulting potential energy curves can be usefully employed to analyse the spectra dealing with transitions involving mixing of singlet and triplet states.

There has been a long interest in experimental and theoretical studies of heteronuclear alkali dimer molecules, since they are relatively simple electronic systems whose molecular spectra coming from low-lying states can be precisely resolved. Moreover, the permanent electric dipole moment makes them one of the best candidates for slowing and trapping using inhomogeneous electric fields, hence enabling to study quantum phenomena such as Bose condensation and Fermi superfluidity [3].

In the past twenty years, several spectroscopic studies on the NaRb dimer were reported. Experiments used different techniques like polarization labeling spectroscopy [4], Fourier transform spectroscopy of laser induced fluorescence supported by deperturbation treatment [5,6], Doppler-free optical–optical double resonance polarization spectroscopy [7], and very recently stimulated Raman adiabatic passage [1,2].

Theoretical studies of the electronic structure of NaRb include the application of many-body multipartitioning perturbation theory [8], configuration interaction by perturbation of the multiconfiguration wave function method [9–11], and our recent calculations based on the multiconfigurational complete active space self-consistent field and multireference configuration interaction methods [12].

Calculations including spin-orbit effects on potential energy curves of alkali dimers can be divided into two groups depending on methods and program packages used. The results on KRb [13], KRb^+ [14], KCs [15], NaCs [16], LiCs [17], LiRb [18] and NaK [19] were obtained using the CIPSI package of Toulouse, dealing with relativistic spin-orbit effects by means of semiempirical spin-orbit pseudopotentials added to the one-component Hamiltonian. The diatomic molecule was treated as a two-electron system where the interaction between electrons and atomic cores was described through non-relativistic or relativistic pseudopotentials. The polarization of the cores was taken into account by using parametrized

https://doi.org/10.1016/j.chemphys.2017.10.005

Post-print of: Wiatr M., Jasik P., Kilich T., Sienkiewicz J., Stoll H.: Quasirelativistic potential energy curves and transition dipole moments of NaRb. CHEMICAL PHYSICS. Vol. 500, (2018), p. 80-87. DOI: 10.1016/j.chemphys.2017.10.005

polarization potentials often taken as l-dependent functions. The only available theoretical results on NaRb with included spin-orbit coupling were performed by Korek et al. [20] who used the above methods with nonempirical relativistic effective pseudopotentials and l-dependent spin-orbit pseudopotentials to reproduce the experimental fine-structure splitting. The full valence configuration-interaction (CI) method with perturbative treatment of spin-orbit effects was applied.

Two other theoretical calculations on KRb [21] and KCs [22] used the MOLPRO code [23] with spin-average small-core pseudopotentials explicitly treating nine valence electrons of each atom. The molecular orbitals were calculated by the complete-active-space self-consistent-field (CASSCF) method, with subsequent multireference CI and separate spin-orbit CI (SOCI).

Our aim is to provide with an alternative quasirelativistic approach, reliable results on electronic states and, for the first time, transition dipole moments for transitions which couple the ground and first excited states with other excited states. In comparison with the other approach [20] we extend the range of internuclear distances up to very large values (86 a_0). Our quasirelativistic calculations include both spin-orbit interaction and scalar relativistic effects, in a model which is based on two-component large-core pseudopotentials supported by core-polarization potentials with carefully chosen basis functions. Thus, NaRb is treated as a two-valence-electron molecule, where an adequate level of correlation can be achieved with relatively low cost. Such an approach may be also applied to triatomic alkali molecules and to alkali clusters.

In Section 2, we describe the computational method used to calculate the electronic structure and transition dipole moments. The results are presented and discussed in Section 3. Conclusions can be found in Section 4.

2. Method

In our computational approach, the alkali metal diatomic is considered as an effective two-electron system. Each atom is replaced by one valence electron and the core consisting of a point nucleus and the remaining electrons from the closed atomic subshells. Since the theoretical approach, without spin-orbit coupling, has been already presented in our earlier papers [12,24–28], here we give only salient details concerning the spin-orbit pseudopotential and atomic basis sets. The calculations are based on the multireference configuration interaction (MRCI) method with large-core atomic effective core potentials (ECP) supplemented by core polarization potentials (CPP), which are vital when explicitly treating only two valence electrons of the NaRb dimer. A rich atomic orbital basis allows to obtain reliable results of the potential energy curves of chosen molecular states. The calculations of the potentials and transition dipole moments are performed by means of the MOLPRO program package [23], while all spectroscopic parameters are obtained by the Level16 program [29]. The core electrons of the sodium atom are represented by the ECP10SDF pseudopotential [30]. In the case of the s and p functions, we use the basis set for sodium which comes with the ECP10SDF pseudopotential. In turn, for the d and f functions we use the cc-pVQZ basis set [31]. Additionally, these basis sets are augmented by thirteen s functions, six p functions, seven d functions, and two f functions. For the rubidium atom, the core electrons are represented by the quasirelativistic effective core pseudopotential ECP36SDF [32]. Here, the set of s and p functions [33,34] coming with the ECP36SDF pseudopotential is expanded by the set of d and f functions coming with the effective core potential ECP28MDF [35] and augmented by thirteen s functions, six p functions, seven d functions, and two f functions. All basis functions were carefully optimized in order to decrease the difference between the calculated atomic asymptotes and the experimental ones. All exponents of our extended and optimized Gaussian basis sets can be found in our earlier paper [12].

While scalar relativistic effects are described by the energy-consistent effective core pseudopotentials, the spin-orbit operator is included by means of spin-orbit pseudopotentials, also implemented in MOLPRO, which have the following l-dependent form [36]

$$V_{SO,\lambda} = \sum_{i,l} \frac{2\Delta V_{i,\lambda l}}{2l+1} P_{\lambda l} \mathbf{s_i} \cdot \mathbf{l_i} P_{\lambda l}, \quad (1)$$

where $P_{\lambda l} = \sum_{m=-l}^{l} |\lambda lm><\lambda lm|$ is the projection operator onto the Hilbert subspace of angular symmetry l with respect to core λ, i indicates the i-th valence electron of the molecule, and l is the orbital quantum number. Here, the index λ, assigned Na or Rb, goes over the atomic cores of the sodium and rubidium atoms. The difference $\Delta V_{i,\lambda l}$ of the radial parts of the two-component pseudopotentials $V_{\lambda l,l+1/2}$ and $V_{\lambda l,l-1/2}$ is given in terms of Gaussians functions

$$\Delta V_{i,\lambda l} = \sum_k A_{\lambda,lk} exp(-a_{\lambda,lk} r_{\lambda i}^2). \quad (2)$$

The spin-orbit pseudopotential parameters $A_{\lambda,lk}$ and $a_{\lambda,lk}$ for sodium and rubidium are given by Soorkia et al. [37] and Silberbach et al. [32], respectively. In the latter case, we modified two parameters, namely $A_{Rb,11}$ and $A_{Rb,12}$ in order to have better adjustments with the experimental values of the spin-orbit splitting (Table 1). The calculated spin-orbit matrix elements are added to the Hamiltonian matrix at the MRCI level.

The potential energy curves and transition dipole moment functions are computed using state-averaged multiconfigurational self-consistent field/complete active space self-consistent field (MCSCF/CASSCF) method to generate the orbitals for the subsequent MRCI calculations. The corresponding active space involves the molecular counterparts of the 3s, 3p and 4s valence orbitals of sodium as well as the 5s, 5p, 4d, 6s, 6p, 5d and 7s valence orbitals of rubidium. Thus, altogether 24 spd orbitals are included in our calculations. Scalar-relativistic MRCI states are used for setting up the Hamiltonian matrix. Finally, the latter is diagonalized after adding the corresponding SO matrix elements.

3. Results and discussion

3.1. Potential energy curves

The molecular calculations were performed for internuclear distances R in the range from 4.6 to 86 a_0 with different step sizes. The calculated potential energy curves correlate for infinite R with fourteen combinations of atomic states including the ground state and thirteen consecutively excited states. We routinely check the quality of our basis sets by performing CI calculations for the ground and excited states of both atoms. In Table 2, the present asymptotic energies show very good and consistent agreement with the experimental atomic levels compiled by Sansonetti [38,39], while Korek and Fawwaz [20] achieved very good agreement only for the first four excited levels of Rb.

Table 1
The spin-orbit pseudopotential parameters (in atomic units) for the Rb atom from Silberbach et al. [32] with two modified $A_{Rb,11}$ and $A_{Rb,12}$ parameters.

lk	11	12	21	22
$A_{Rb,lk}$	−2.9502	2.8551	1.9574	−1.8972
$a_{Rb,lk}$	0.31777	0.30313	0.37996	0.37277

Post-print of: Wiatr M., Jasik P., Kilich T., Sienkiewicz J., Stoll H.: Quasirelativistic potential energy curves and transition dipole moments of NaRb. CHEMICAL PHYSICS. Vol. 500, (2018), p. 80-87. DOI: 10.1016/j.chemphys.2017.10.005

Table 2
The comparison of the asymptotic energies of the electronic states with the other theoretical and experimental results. Δ_{S-p} and Δ_{S-K} stand for differences between experimental values provided by Sansonetti [38,39] and present as well as Korek and Fawwaz [20] results, respectively. Energies are shown in cm^{-1} units. The capital letter T refers to theoretical results and E denotes experimental data.

Asymptotes	Electronic states	present T	Sansonetti E	Korek and Fawwaz T	Δ_{S-p}	Δ_{S-K}
Na(3s $^2S_{1/2}$) + Rb(5s $^2S_{1/2}$)	$(1)0^+$, $(1)0^-$, (1)1					
Na(3s $^2S_{1/2}$) + Rb(5p $^2P_{1/2}$)	$(2)0^+$, $(2)0^-$, (2)1	12579.55	12578.95	12578.32	−0.60	0.63
Na(3s $^2S_{1/2}$) + Rb(5p $^2P_{3/2}$)	$(3)0^+$, $(3)0^-$, (3,4)1, (1)2	12818.89	12816.55	12815.99	−2.34	0.56
Na(3p $^2P_{1/2}$) + Rb(5s $^2S_{1/2}$)	$(4)0^+$, $(4)0^-$, (5)1	16953.82	16956.17	16967.48	2.35	−11.31
Na(3p $^2P_{3/2}$) + Rb(5s $^2S_{1/2}$)	$(5)0^+$, $(5)0^-$, (6,7)1, (2)2	16973.64	16973.37	17004.41	−0.27	−31.04
Na(3s $^2S_{1/2}$) + Rb(4d $^2D_{5/2}$)	$(6)0^+$, $(6)0^-$, (8,9)1, (3,4)2, (1)3	19357.39	19355.20	19354.87	−2.19	0.33
Na(3s $^2S_{1/2}$) + Rb(4d $^2D_{3/2}$)	$(7)0^+$, $(7)0^-$, (10,11)1, (5)2	19358.05	19355.65	19354.87	−2.40	0.78
Na(3s $^2S_{1/2}$) + Rb(6s $^2S_{1/2}$)	$(8)0^+$, $(8)0^-$, (12)1	20128.54	20132.51	20101.35	3.97	31.16
Na(3s $^2S_{1/2}$) + Rb(6p $^2P_{1/2}$)	$(9)0^+$, $(9)0^-$, (13)1	23713.37	23715.08	23748.14	1.71	−33.06
Na(3s $^2S_{1/2}$) + Rb(6p $^2P_{3/2}$)	$(10)0^+$, $(10)0^-$, (14,15)1, (6)2	23790.91	23792.59	23825.73	1.68	−33.14
Na(3s $^2S_{1/2}$) + Rb(5d $^2D_{3/2}$)	$(11)0^+$, $(11)0^-$, (16,17)1, (7)2	25698.73	25700.54	25707.75	1.81	−7.21
Na(3s $^2S_{1/2}$) + Rb(5d $^2D_{5/2}$)	$(12)0^+$, $(12)0^-$, (18,19)1, (8,9)2, (2)3	25701.57	25703.50	25710.72	1.93	−7.22
Na(4s $^2S_{1/2}$) + Rb(5s $^2S_{1/2}$)	$(13)0^+$, $(13)0^-$, (20)1	25737.57	25740.00	25760.09	2.43	−20.09
Na(3s $^2S_{1/2}$) + Rb(7s $^2S_{1/2}$)	$(14)0^+$, $(14)0^-$, (21)1	26307.64	26311.44	26300.98	3.80	10.46

Our results of potential energy curves are displayed in Figs. 1–4. In Fig. 1, the potential energy curve of the $(1)0^+$ ground state has the shape of the Morse potential. An important feature for the photoassociation process is the avoided crossing between the potential energy curves of the $(2)0^+$ and $(3)0^+$ states which takes place around 7.8 a_0. It results in the double well of the lower curve and subsequently in the irregular spacings of vibrational levels. The upper curve assumes the shape of the Morse potential. Another interesting feature is the interaction between potential curves of the $(4)0^+$ and $(5)0^+$ states which respectively correlate with $P_{1/2}$ and $P_{3/2}$ of sodium doublet. This interaction leads to avoided crossings at R = 13.8 and 18.4 a_0. The wavy shape of the $(5)0^+$ potential energy curve comes from several avoiding crossings with the higher $(6)0^+$ potential energy curve correlating with the Na(3s $^2S_{1/2}$) + Rb(4*d* $^2D_{5/2}$) atomic asymptote. The situation is similar for all higher excited 0^+ states, which makes them very irregular potentials.

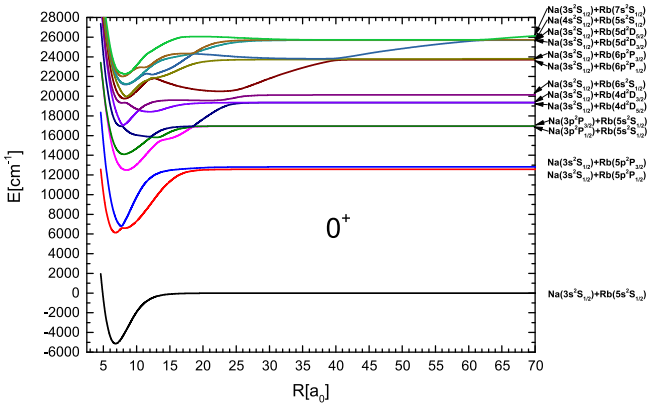

Fig. 1. Quasirelativistic potential energy curves of the fourteen $\Omega = 0^+$ states.

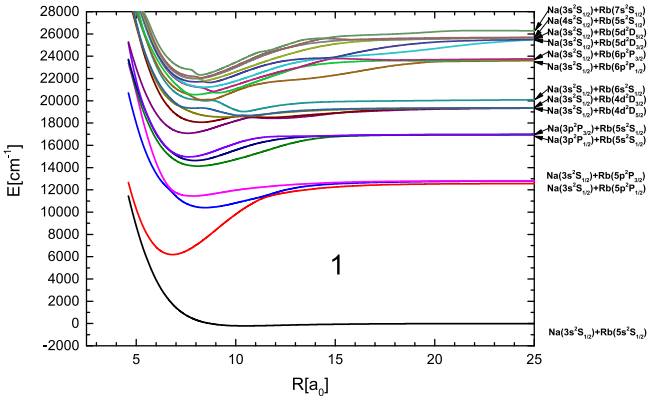

Fig. 3. Quasirelativistic potential energy curves of the twenty-one $\Omega = 1$ states.

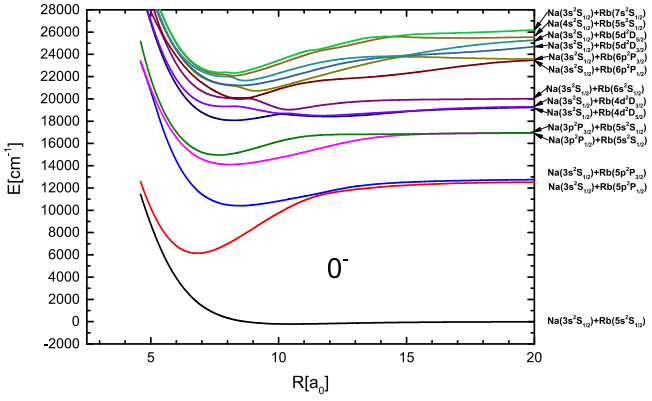

Fig. 2. Quasirelativistic potential energy curves of the fourteen $\Omega = 0^-$ states.

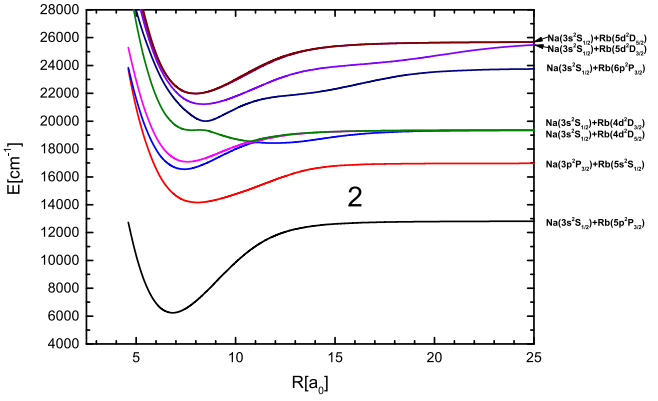

Fig. 4. Quasirelativistic potential energy curves of the nine $\Omega = 2$ states.

Post-print of: Wiatr M., Jasik P., Kilich T., Sienkiewicz J., Stoll H.: Quasirelativistic potential energy curves and transition dipole moments of NaRb. CHEMICAL PHYSICS. Vol. 500, (2018), p. 80-87. DOI: 10.1016/j.chemphys.2017.10.005

The presently calculated spectroscopic parameters along with ones from the theoretical work of Korek and Fawwaz [20] as well as results derived from the experiment using deperturbation techniques given by Docenko et al. [6] are shown in Table 3.

The most important differences between these three sets of parameters are connected with the double minimum of the $(2)0^+$ state arising due to the avoided crossing with the $(3)0^+$ state. The outer well of this potential in the Hund's case (c) corresponds to $A^1\Sigma^+$ in the Hund's case (a), while the inner well is an equivalent to $b^3\Pi$. It should be noticed that in the Hund's case (a) the considered potential energy curves of the NaRb molecule correlate in the asymptotic region to the center of the multiplet Rb($5p\ ^2P$), while in the Hund's case (c) proper atomic limits are Rb($5p\ ^2P_{1/2}$) and Rb($5p\ ^2P_{3/2}$). Only limited comparison between the spectroscopic parameters coming from these two representations can be performed. For the equilibrium length R_e, differences between the experimental value of Docenko [6] and present as well as Korek and Fawwaz [20] results amount to 0.095 and 0.115 a_0, respectively. The present dissociation energy D_e of the outer well of the $(2)0^+$ state equals to 5989 cm^{-1}, whereas Korek and Fawwaz [20] do not determine this parameter. The relative depth of the outer well of the $(2)0^+$ state, taken as a difference between the top of the barrier and the minimum value, equals to 53 cm^{-1}. The same parameter given by Korek and Fawwaz [20] amounts only to 29 cm^{-1}. In our case, the well depth is sufficient to localize rovibrational levels and allows to determine vibrational constant ω_e = 65.17 cm^{-1} and rotational constant B_e = 0.05054 cm^{-1}.

The case of the inner well of the $(2)0^+$ state is more complicated, because of the existence of additional potential energy curves of the $(2)0^-$, $(2)1$, and $(1)2$ states. The splitting between these potentials around the minimum of the inner well almost exactly obeys the formula for the electronic energy of a multiplet term $T_e = T_0 + A^{SO}\Lambda\Sigma$, where T_0 is the term value when the spin is neglected, Λ is the component of the electronic orbital angular momentum along the internuclear axis, and A^{SO} is the spin-orbit constant for a given multiplet term [40]. The values of A^{SO} in the considered system are 50.6 and 49.1 cm^{-1} for $E^{(2)1}(R_e) - E^{(2)0^+}(R_e)$ and $E^{(1)2}(R_e) - E^{(2)1}(R_e)$, respectively. These parameters are in good agreement with the results given by Korek and Fawwaz [20], which are equal to 50.9 and 48.2 cm^{-1}, respectively. We are able to compare the present spectroscopic parameters of the inner well of the $(2)0^+$ and $(2)0^-$ states with the component $\Omega = 0$ of the $b^3\Pi$ state reported by Docenko et al. [6]. For instance, differences between the experimental value of the equilibrium length R_e and ours is around 0.05 a_0 and is twice as small as the difference between the experimental value and the result given by Korek et al. [20]. It is visible from Tables 3 and 4, that the present dissociation energies D_e calculated for the inner well of the $(2)0^+$ and $(2)0^-$ states are respectively 73 and 71 cm^{-1} larger in the comparison with the value reported by Docenko et al. [6]. The same well depths given by Korek and Fawwaz [20] are respectively deeper by 200 and 199 cm^{-1} than the experimental value. It can be noticed that in the asymptotic region the $b^3\Pi_0$ state reported by Docenko et al. correlates with Rb($5p^2P_{1/2}$) + ξ^{so}_{Rb} instead with Rb($5p^2P_{1/2}$). Our rubidium spin-orbit splitting $\xi^{so}_{Rb} = [E_{5p^2P_{3/2}} - E_{5p^2P_{1/2}}]/3$ is equal to 79.78 cm^{-1} and agrees very well with experimental data provided by Sansonetti (79.20 cm^{-1}) [38,39] and Docenko et al. (79.22 cm^{-1}) [6].

The rich structure of the potential energy curves of the $\Omega = 0^-$ states are presented in Fig. 2. The lowest avoided crossings take

Table 3
The spectroscopic parameters of the bond length R_e (a_0), the dissociation energy D_e, the vertical transition energy T_{ev}, the electronic term energy T_e, the vibrational constant ω_e, the rotational constant B_e and the bond energy D_0 (all in cm^{-1}) for the ground and chosen excited states of the 0^+ symmetry.

State	Asymptote	R_e	D_e	T_{ev}	T_e	ω_e	B_e	D_0	
$(1)0^+$	Na($3s\ ^2S_{1/2}$) + Rb($5s\ ^2S_{1/2}$)	6.83	5141		0	106.67	0.07094	5088	present
		6.78	5263		0	107.90	0.07228		[20]
$(2)0^+$	Na($3s\ ^2S_{1/2}$) + Rb($5p\ ^2P_{1/2}$)	6.82	6451	11216	11270	103.92	0.07117	6399	present
		6.77	6578		11259	105.70	0.07259		[20]
$b^3\Pi_0$	Na($3s\ ^2S_{1/2}$) + Rb($5p\ ^2P_{1/2}$ + ξ^{so}_{Rb})	6.869	6378		11361				[6]
barrier		7.83			11784				present
		7.80			11794				[20]
second min.		8.22	5989		11731	65.17	0.05054	5957	present
		8.20			11765				[20]
$A^1\Sigma^+$	Na(3s) + Rb(5p)	8.315	6080		11688				[6]
$(3)0^+$	Na($3s\ ^2S_{1/2}$) + Rb($5p\ ^2P_{3/2}$)	7.71	6061	12726	11899	174.70	0.05621	5973	present
$(4)0^+$	Na($3p\ ^2P_{1/2}$) + Rb($5s\ ^2S_{1/2}$)	8.46	4455	18785	17640	63.33	0.04621	4423	present
		8.34	4525		17705	64.90	0.04774		[20]
$(5)0^+$	Na($3p\ ^2P_{3/2}$) + Rb($5s\ ^2S_{1/2}$)	8.09	2868	19886	19246	61.65	0.05040	2838	present
		7.94	2968		19261	78.60	0.05266		[20]
$(9)0^+$	Na($3s\ ^2S_{1/2}$) + Rb($6p\ ^2P_{1/2}$)	8.18	3957	25865	24897	70.78	0.04934	3922	present
		8.13	4067		24941	72.00	0.05031		[20]
$(10)0^+$	Na($3s\ ^2S_{1/2}$) + Rb($6p\ ^2P_{3/2}$)	8.47	3826	26841	25106	110.45	0.04603	3771	present
		8.40	3962		25126	118.50	0.04709		[20]
$(11)0^+$	Na($3s\ ^2S_{1/2}$) + Rb($5d\ ^2D_{3/2}$)	8.36	4513	27367	26327	63.39	0.04724	4481	present
		8.30			26439	62.90	0.04822		[20]
barrier		11.51			27431				present
		11.50			27576				[20]
second min.		12.36	3506		27333	63.58	0.02177	3474	present
		12.30	3112		27498				[20]
$(12)0^+$	Na($3s\ ^2S_{1/2}$) + Rb($5d\ ^2D_{5/2}$)	8.41	4457	27407	26385	60.01	0.04678	4427	present
		8.30	4495		26475	61.60	0.04829		[20]
$(13)0^+$	Na($4s\ ^2S_{1/2}$) + Rb($5s\ ^2S_{1/2}$)	7.90	3739	27760	27139	80.34	0.05276	3699	present
		7.87	3752		27222	79.50	0.05368		[20]
$(14)0^+$	Na($3s\ ^2S_{1/2}$) + Rb($7s\ ^2S_{1/2}$)	8.20	4055	28049	27394	71.03	0.04909	4019	present
		8.14	3558		27463	72.80	0.05022		[20]

Post-print of: Wiatr M., Jasik P., Kilich T., Sienkiewicz J., Stoll H.: Quasirelativistic potential energy curves and transition dipole moments of NaRb. CHEMICAL PHYSICS. Vol. 500, (2018), p. 80-87. DOI: 10.1016/j.chemphys.2017.10.005

Table 4
The spectroscopic parameters of the bond length R_e (a_0), the dissociation energy D_e, the vertical transition energy T_{ev}, the electronic term energy T_e, the vibrational constant ω_e, the rotational constant B_e and the bond energy D_0 (all in cm^{-1}) for the chosen excited states of the 0^- symmetry.

State	Asymptote	R_e	D_e	T_{ev}	T_e	ω_e	B_e	D_0	
$(1)0^-$	$Na(3s\ ^2S_{1/2}) + Rb(5s\ ^2S_{1/2})$	10.50	210	6815	4931	20.17	0.02966	200	present
		10.22	284		4979	22.40	0.03183		[20]
$(2)0^-$	$Na(3s\ ^2S_{1/2}) + Rb(5p\ ^2P_{1/2})$	6.81	6449	11218	11272	104.19	0.07121	6397	present
		6.77	6577		11263	105.90	0.07261		[20]
$(3)0^-$	$Na(3s\ ^2S_{1/2}) + Rb(5p\ ^2P_{3/2})$	8.47	2409	16850	15550	61.72	0.04598	2379	present
		8.41	2444		15635	62.60	0.04696		[20]
$(4)0^-$	$Na(3p\ ^2P_{1/2}) + Rb(5s\ ^2S_{1/2})$	8.09	2849	19885	19245	61.68	0.05041	2818	present
		8.13	2956		19288	46.40	0.04976		[20]
$(5)0^-$	$Na(3p\ ^2P_{3/2}) + Rb(5s\ ^2S_{1/2})$	7.65	2017	20456	20098	79.17	0.05642	1977	present
		7.59	2130		20104	79.40	0.05763		[20]
$(6)0^-$	$Na(3s\ ^2S_{1/2}) + Rb(4d\ ^2D_{5/2})$	8.22	1286	24135	23212	65.21	0.04882	1253	present
		8.16			23227	66.40	0.04988		[20]
barrier		10.10			23786				present
		10.20			23860				[20]
second min.		11.94	939		23559	29.92	0.02327	924	present
		11.59	2384		23654	65.30	0.02476		[20]
$(10)0^-$	$Na(3s\ ^2S_{1/2}) + Rb(6p\ ^2P_{3/2})$	9.10	3086	27298	25846	110.45	0.03973	3030	present
		9.06	3137		25945	114.40	0.04046		[20]
$(11)0^-$	$Na(3s\ ^2S_{1/2}) + Rb(5d\ ^2D_{3/2})$	8.44	4495	27402	26344	76.09	0.04624	4457	present
		8.30	4511		26460	63.20	0.04821		[20]
$(14)0^-$	$Na(3s\ ^2S_{1/2}) + Rb(7s\ ^2S_{1/2})$	8.23	4019	28049	27429	151.60	0.04942	3943	present
		8.18	4045		27500	177.50	0.04960		[20]

place between $(2)0^-$ and $(3)0^-$ at 11.8 a_0, and between $(4)0^-$ and $(5)0^-$ at 6.0 and 16.6 a_0. The states in the 0^- symmetry have more regular shapes compared to 0^+ states. Some of our spectroscopic parameters differ quite substantially from these of Korek and Fawwaz [20] (see Table 4). This is particularly visible in the case of the dissociation energy D_e where for the lowest $(1)0^-$ state the difference equals to 74 cm^{-1}. The bond length of this state also differs from the one reported in Ref. [20] by 0.28 a_0 towards the larger internuclear distances. The comparison of ω_e parameters indicates that the presently reported $(1)0^-$ state is slightly broader, because our vibrational constant is smaller.

Potential energy curves of twenty-one $\Omega = 1$ states are given in Fig. 3, where the avoided crossings between (2), (3) and (4)1 states are clearly visible and may be found important in the photoassociation experiments. The higher states are again not regular, due to many avoided crossings. In the case of the double well (8)1 state,

Table 5
The spectroscopic parameters of the bond length R_e (a_0), the dissociation energy D_e, the vertical transition energy T_{ev}, the electronic term energy T_e, the vibrational constant ω_e, the rotational constant B_e and the bond energy D_0 (all in cm^{-1}) for the chosen excited states of the 1 symmetry.

State	Asymptote	R_e	D_e	T_{ev}	T_e	ω_e	B_e	D_0	
(1)1	$Na(3s\ ^2S_{1/2}) + Rb(5s\ ^2S_{1/2})$	10.50	210	6816	4931	20.17	0.02966	200	present
		10.22	284		4979	22.60	0.03186		[20]
(2)1	$Na(3s\ ^2S_{1/2}) + Rb(5p\ ^2P_{1/2})$	6.82	6400	11267	11320	104.16	0.07111	6348	present
		6.76	6530		11310	106.00	0.07269		[20]
(3)1	$Na(3s\ ^2S_{1/2}) + Rb(5p\ ^2P_{3/2})$	8.47	2413	16829	15547	61.63	0.04598	2382	present
		8.41	2444		15634	62.50	0.04696		[20]
(4)1		7.82	1373	16987	16586	61.90	0.05383	1342	present
		7.77	1445		16634	62.40	0.05510		[20]
(5)1	$Na(3p\ ^2P_{1/2}) + Rb(5s\ ^2S_{1/2})$	8.08	2821	19909	19274	61.77	0.05048	2790	present
		8.00	2928		19303	63.40	0.05200		[20]
(6)1	$Na(3p\ ^2P_{3/2}) + Rb(5s\ ^2S_{1/2})$	7.95	2342	20401	19773	73.19	0.05223	2305	present
		7.86	2381		19849	74.60	0.05381		[20]
(7)1		7.65	2017	20457	20098	79.18	0.05642	1977	present
		7.59	2126		20105	81.70	0.05765		[20]
(8)1	$Na(3s\ ^2S_{1/2}) + Rb(4d\ ^2D_{5/2})$	7.58	2274	22492	22224	76.11	0.05737	2236	present
		7.56	2281		22336	75.80	0.05820		[20]
barrier		10.79			23657				present
		10.70			23761				[20]
second. min.		11.95	934		23564	30.03	0.02321	919	present
		11.88			23668	30.40	0.02355		[20]
(9)1	$Na(3s\ ^2S_{1/2}) + Rb(4d\ ^2D_{5/2})$	8.22	1286	24135	23212	65.21	0.04882	1253	present
		8.16	1391		23227	66.10	0.04987		[20]
(16)1	$Na(3s\ ^2S_{1/2}) + Rb(5d\ ^2D_{3/2})$	8.43	4486	27430	26354	73.14	0.04662	4449	present
		8.28	4494		26743	63.70	0.04848		[20]
(19)1	$Na(3s\ ^2S_{1/2}) + Rb(5d\ ^2D_{5/2})$	7.85	3693	27818	27150	43.54	0.05146	3671	present
		8.05	3726		27266	75.70	0.05107		[20]
(20)1	$Na(4s\ ^2S_{1/2}) + Rb(5s\ ^2S_{1/2})$	8.23	3700	27963	27179	168.15	0.04865	3616	present
		8.16	3727		27316	94.90	0.04995		[20]
(21)1	$Na(3s\ ^2S_{1/2}) + Rb(7s\ ^2S_{1/2})$	8.19	4015	28509	27433	157.03	0.04854	3937	present
		8.19	4045		27498	180.90	0.04947		[20]

Post-print of: Wiatr M., Jasik P., Kilich T., Sienkiewicz J., Stoll H.: Quasirelativistic potential energy curves and transition dipole moments of NaRb. CHEMICAL PHYSICS. Vol. 500, (2018), p. 80-87. DOI: 10.1016/j.chemphys.2017.10.005

Table 6
The spectroscopic parameters of the bond length R_e (a_0), the dissociation energy D_e, the vertical transition energy T_{ev}, the electronic term energy T_e, the vibrational constant ω_e, the rotational constant B_e and the bond energy D_0 (all in cm^{-1}) for the chosen excited states of the 2 symmetry.

State	Asymptote	R_e	D_e	T_{ev}	T_e	ω_e	B_e	D_0	
(1)2	Na(3s $^2S_{1/2}$) + Rb(5p $^2P_{3/2}$)	6.82	6591	11316	11369	104.15	0.07101	6539	present
		6.76	6720		11358	106.20	0.07277		[20]
(2)2	Na(3p $^2P_{3/2}$) + Rb(5s $^2S_{1/2}$)	8.08	2812	19934	19302	61.80	0.05052	2781	present
		8.00	2900		19331	63.20	0.05190		[20]
(3)2	Na(3s $^2S_{1/2}$) + Rb(4d $^2D_{5/2}$)	7.40	2811	21828	21687	80.43	0.06024	2771	present
		7.36	2836		21782	80.30	0.06131		[20]
barrier		11.02			23634				present
		11.00			23735				[20]
second min.		11.97	930		23568				present
		11.90			23676				[20]
(4)2	Na(3s $^2S_{1/2}$) + Rb(4d $^2D_{5/2}$)	7.59	2274	22492	22224	76.10	0.05737	2236	present
		7.56	2279		22339	75.70	0.05819		[20]
(6)2	Na(3s $^2S_{1/2}$) + Rb(6p $^2P_{3/2}$)	8.48	3796	26870	25136	110.76	0.04594	3741	present
		8.42	3912		25178	115.60	0.04691		[20]
(7)2	Na(3s $^2S_{1/2}$) + Rb(5d $^2D_{3/2}$)	8.36	4477	27463	26363	64.82	0.04724	4444	present
		8.27	4483		26488	64.60	0.04857		[20]
(8)2	Na(3s $^2S_{1/2}$) + Rb(5d $^2D_{5/2}$)	7.97	3728	27804	27115	74.01	0.05201	3691	present
		7.87	3746		27226	79.10	0.05371		[20]
(9)2	Na(3s $^2S_{1/2}$) + Rb(5d $^2D_{5/2}$)	8.00	3716	27824	27126	71.11	0.05177	3681	present
		7.92	3692		27283	72.60	0.05289		[20]

contrarily to Korek and Fawwaz, we find two substantial depths. The spectroscopic parameters of the $\Omega = 1$ states are shown in Table 5. Regarding the (1)1 potential energy curve, all parameters have the same values as for the $(1)0^-$ state, so the comparative analysis for this potential with data provided by Korek and Fawwaz is analogous. These two potentials, $(1)0^-$ and (1)1, are often adjusted by applying an adequate magnetic field in order to achieve the Feshbach resonance with the chosen excited states. In the case of the (2)1 state, the presently reported dissociation energy D_e is equal to 6530 cm^{-1}, while in Ref. [20] the same property equals 6400 cm^{-1}. The electronic term energy T_e is similar in the both data sets and the difference amounts to 10 cm^{-1} only. The agreement of the present R_e, ω_e and B_e parameters in the comparison with those provided by Korek et al. [20] is quite reasonable. The (2)1 potential, together with the complex of $(2, 3)0^+$ states, can play an important role in the creation of cold NaRb molecules in the deeply bound ground state.

In the case of $\Omega = 2$ states (Fig. 4), the shapes of potential energy curves are rather regular. However, the most interesting feature is the avoided crossing at 11.0 a_0 involving three potential energy curves of (3), (4) and (5)2 states. The spectroscopic parameters are presented in Table 6 where D_e again shows the biggest disagreement with Korek and Fawwaz reaching 129 cm^{-1} for the lowest (1)2 state. Additionally, the figure with the two calculated curves of the $\Omega = 3$ states can be found in the Supplementary materials.

A general comparison between our results and those of Korek and Fawwaz [20] shows that almost all their potential energy curves have deeper wells (D_e) than ours and consequently in the same cases their equilibrium bond lengths (R_e) are shorter than ours. Moreover, quite systematically, their electronic term energies T_e, vibrational constants ω_e and rotational constants B_e are larger than obtained in our calculations. The above discrepancies can be assigned to different codes used which employ different effective core and polarization pseudopotentials. Also different basis sets were used in the two computational approaches.

3.2. Transition dipole moments

In Figs. 5 and 6, we present, calculated for the first time, the squares of quasirelativistic transition dipole moments of the NaRb molecule. The transitions from the ground $(1)0^+$ state to the consecutive five excited states of the same symmetry are given in Fig. 5. Generally, transition dipole moments are sharp and irregular along the internuclear separation R. A characteristic switch between the values of different pairs occurs at the exact points of avoiding crossings. For instance, it occurs at R = 7.8 a_0 between the transitions to $(2)0^+$ and $(3)0^+$. In the range of R from 8 a_0 to 20 a_0 the transition to the lowest excited state $(2)0^+$ clearly dominates and evidently can be used in photoassociation experiments. Behind R = 20 a_0 the transition to $(3)0^+$ possesses a larger value. In Fig. 6, we display the squares of transition dipole moments from the ground state to the six consecutive excited states of 1 symmetry. Worth noticing are the relatively small values of the atomic resonance transition to the low lying (2)1 state along the covered internuclear separation R. Besides the transitions from the ground state, the knowledge of transitions from the Feshbach states $(1)0^-$ and 1 (1) is very important for planned experiments. Figures with these transitions can be found in the Supplementary materials.

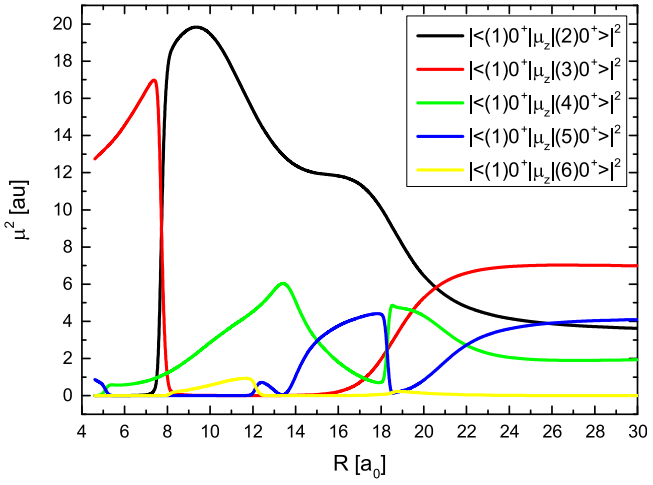

Fig. 5. Squares of the transition dipole moments between the ground state and five low-lying 0^+ states.

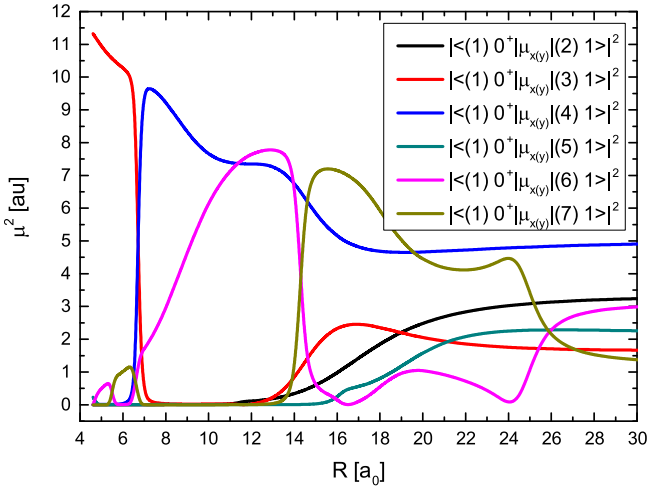

Fig. 6. Squares of the transition dipole moments between the ground state and six 1 states.

4. Conclusion

This paper presents results of quasirelativistic calculations of adiabatic Born–Oppenheimer potential energy curves and, for the first time, quasirelativistic transition dipole moments of the NaRb molecule. In our computational approach, two valence electrons are taken explicitly into account for building determinants for the multiconfiguration wave function. Atomic cores are described by energy-consistent semi-local pseudopotentials and core polarization potentials. Relativistic effects taken into account include spin-orbit interaction and scalar-relativistic effects. The calculated potential energy curves very accurately correlate with (1) the $^2S_{1/2}$ ground states of the Na and Rb atoms, (2) the ground state 3s $^2S_{1/2}$ of the Na atom and the excited states 5p $^2P_{1/2,3/2}$, 4d $^2D_{5/2,3/2}$, 6s $^2S_{1/2}$, 6p $^2P_{1/2,3/2}$, 5d $^2D_{3/2,5/2}$ and 7s $^2S_{1/2}$ of the Rb atom, and (3) the excited states 3p $^2P_{1/2,3/2}$ and 4s $^2S_{1/2}$ of the Na atom and the ground state 5s $^2S_{1/2}$ of the Rb atom. Several new features of quasirelativistic potential energy curves are described, among them very important avoided crossings between low-lying potentials of the states with 0^+, 0^- and 1 symmetries. The large set of spectroscopic parameters is presented and compared with available experimental and theoretical results. The representative features of the quasirelativistic transition dipole moments are shown in connection with the sudden change of theirs values around the regions, in which the avoided crossings between appropriate potentials exist.

Acknowledgements

We thank Olivier Dulieu, Wlodzimierz Jastrzebski, Pawel Kowalczyk, and Jacek Szczepkowski for useful discussion. We acknowledge partial support by the COST Action CM1204 of the European Community and the Polish Ministry of Science and Higher Education. Calculations have been carried out using resources provided by Academic Computer Centre in Gdansk and Wroclaw Centre for Networking and Supercomputing.

Appendix A. Supplementary data

See supplementary material for pointwise quasirelativistic adiabatic potential energy curves and squares of nonvanishing components of transition dipole moments related to all figures presented in this article. Supplementary data associated with this article can be found, in the online version, athttps://doi.org/10.1016/j.chemphys.2017.10.005.

References

[1] M. Guo, B. Zhu, B. Lu, X. Ye, F. Wang, R. Vexiau, N. Bouloufa-Maafa, G. Quéméner, O. Dulieu, D. Wang, Creation of an ultracold gas of ground-state dipolar $^{23}Na^{87}Rb$ molecules, Phys. Rev. Lett. 116 (2016) 205303, https://doi.org/10.1103/PhysRevLett.116.205303.

[2] B. Zhu, X. Li, X. He, M. Guo, F. Wang, R. Vexiau, N. Bouloufa-Maafa, O. Dulieu, D. Wang, Long-range states of the NaRb molecule near the $Na(3\,^2S_{1/2}) + Rb(5\,^2P_{3/2})$ asymptote, Phys. Rev. A 93 (2016) 012508, https://doi.org/10.1103/PhysRevA.93.012508.

[3] S.A. Moses, J.P. Covey, M.T. Miecnikowski, D.S. Jin, J. Ye, New frontiers for quantum gases of polar molecules, Nat. Phys. 13 (1) (2017) 13–20, https://doi.org/10.1038/nphys3985.

[4] A. Pashov, W. Jastrzębski, P. Kortyka, P. Kowalczyk, Experimental long range potential of the $B^1\Pi$ state in NaRb, J. Chem. Phys. 124 (20) (2006) 204308, https://doi.org/10.1063/1.2198199.

[5] M. Tamanis, R. Ferber, A. Zaitsevskii, E.A. Pazyuk, A.V. Stolyarov, H. Chen, J. Qi, H. Wang, W.C. Stwalley, High resolution spectroscopy and channel-coupling treatment of the $A^1\Sigma^+ - b^3\Pi$ complex of NaRb, J. Chem. Phys. 117 (17) (2002) 7980–7988, https://doi.org/10.1063/1.1505442.

[6] O. Docenko, M. Tamanis, R. Ferber, E.A. Pazyuk, A. Zaitsevskii, A.V. Stolyarov, A. Pashov, H. Knöckel, E. Tiemann, Deperturbation treatment of the $A^1\Sigma^+ - b^3\Pi$ complex of NaRb and prospects for ultracold molecule formation in $X^1\Sigma^+(v = 0; j = 0)$, Phys. Rev. A 75 (2007) 042503, https://doi.org/10.1103/PhysRevA.75.042503.

[7] S. Kasahara, T. Ebi, M. Tanimura, H. Ikoma, K. Matsubara, M. Baba, H. Katô, High resolution laser spectroscopy of the $X^1\Sigma^+$ and $(1)^3\Sigma^+$ states of $^{23}Na^{85}Rb$ molecule, J. Chem. Phys. 105 (4) (1996) 1341–1347, https://doi.org/10.1063/1.472000.

[8] A. Zaitsevskii, S.O. Adamson, E.A. Pazyuk, A.V. Stolyarov, O. Nikolayeva, O. Docenko, I. Klincare, M. Auzinsh, M. Tamanis, R. Ferber, R. Cimiraglia, Energy and radiative properties of the low-lying NaRb states, Phys. Rev. A 63 (2001) 052504, https://doi.org/10.1103/PhysRevA.63.052504.

[9] M. Korek, A. Allouche, M. Kobeissi, A. Chaalan, M. Dagher, K. Fakherddin, M. Aubert-Frécon, Theoretical study of the electronic structure of the LiRb and NaRb molecules, Chem. Phys. 256 (1) (2000) 1–6, https://doi.org/10.1016/S0301-0104(00)00061-6.

[10] R. Dardouri, K. Issa, B. Oujia, F. Xavier Gadéa, Theoretical study of the electronic structure of LiX and NaX (X= Rb, Cs) molecules, Int. J. Quantum Chem. 112 (15) (2012) 2724–2734, https://doi.org/10.1002/qua.23295.

[11] M. Chaieb, H. Habli, L. Mejrissi, B. Oujia, F.X. Gadéa, Ab initio spectroscopic study for the NaRb molecule in ground and excited states, Int. J. Quantum Chem. 114 (11) (2014) 731–747, https://doi.org/10.1002/qua.24664.

[12] M. Wiatr, P. Jasik, J.E. Sienkiewicz, The adiabatic potentials of low-lying electronic states of the NaRb molecule, Phys. Scr. 90 (5) (2015) 054012, http://stacks.iop.org/1402-4896/90/i=5/a=05401.

[13] S. Rousseau, A. Allouche, M. Aubert-Frécon, Theoretical study of the electronic structure of the KRb molecule, J. Mol. Spectrosc. 203 (2) (2000) 235–243, https://doi.org/10.1006/jmsp.2000.8142, http://www.sciencedirect.com/science/article/pii/S0022285200981426.

[14] M. Korek, G. Younes, A.R. Allouche, Theoretical study of the low-lying electronic states of the molecular ion KRb^+, Int. J. Quantum Chem. 92 (4) (2003) 376–380, https://doi.org/10.1002/qua.10485.

[15] M. Korek, Y.A. Moghrabi, A.R. Allouche, Theoretical calculation of the excited states of the KCs molecule including the spin-orbit interaction, J. Chem. Phys. 124 (9) (2006) 094309, https://doi.org/10.1063/1.2173239.

[16] M. Korek, S. Bleik, A.R. Allouche, Theoretical calculation of the low laying electronic states of the molecule NaCs with spin-orbit effect, J. Chem. Phys. 126 (12) (2007) 124313, https://doi.org/10.1063/1.2710257.

[17] N. Elkork, D. Houalla, M. Korek, Theoretical calculation of the electronic states with spin-orbit effects of the molecule LiCs, Can. J. Phys. 87 (10) (2009) 1079–1088, https://doi.org/10.1139/P09-070.

[18] M. Korek, G. Younes, S. AL-Shawa, Theoretical calculation of the electronic structure of the molecule LiRb including the spin-orbit interaction, J. Mol. Struct. (Thoechem.) 899 (1) (2009) 25–31, https://doi.org/10.1016/j.theochem.2008.12.006, http://www.sciencedirect.com/science/article/pii/S0166128008007434.

[19] A.R. Allouche, M. Aubert-Frécon, Ab initio and long-range investigation of the $\Omega^{(+/-)}$ states of NaK dissociating adiabatically up to $Na(3s\,^2S_{1/2}) + K(3d\,^2D_{3/2})$, J. Chem. Phys. 135 (2) (2011) 024309, https://doi.org/10.1063/1.3607964.

[20] M. Korek, O. Fawwaz, Theoretical calculation of the electronic states with spin-orbit effects of the molecule NaRb, Int. J. Quantum Chem. 109 (5) (2009) 938–947, https://doi.org/10.1002/qua.21904.

[21] S.J. Park, Y.J. Choi, Y.S. Lee, G.-H. Jeung, Ab initio calculations of the electronic states of KRb, Chem. Phys. 257 (2) (2000) 135–145, https://doi.org/10.1016/S0301-0104(00)00152-X.

[22] S. Rousseau, A. Allouche, M. Aubert-Frécon, Theoretical study of the electronic structure of the KRb molecule, J. Mol. Spectrosc. 203 (2) (2000) 235–243, https://doi.org/10.1006/jmsp.2000.8142, http://www.sciencedirect.com/science/article/pii/S0022285200981426.

[23] H.-J. Werner, P.J. Knowles, G. Knizia, F.R. Manby, M. Schütz, Molpro: a general-purpose quantum chemistry program package, Wiley Interdisciplinary Rev. Comput. Mol. Sci. 2 (2) (2012) 242–253, https://doi.org/10.1002/wcms.82.

[24] P. Jasik, J.E. Sienkiewicz, Transition dipole moments of the lithium dimer, At. Data Nucl. Data Tables 99 (2) (2013) 115–155, https://doi.org/10.1016/j.adt.2011.06.003, http://www.sciencedirect.com/science/article/pii/S0092640X12000733.

[25] L. Midowicz, P. Jasik, J.E. Sienkiewicz, Possible schemes of photoassociation processes in the KLi molecule with newly calculated potential energy curves, Cent. Eur. J. Phys. 11 (9) (2013) 1115–1122, https://doi.org/10.2478/s11534-013-0199-z.

[26] P. Łobacz, P. Jasik, J.E. Sienkiewicz, Theoretical study of highly-excited states of KRb molecule, Cent. Eur. J. Phys. 11 (9) (2013) 1107–1114, https://doi.org/10.2478/s11534-012-0137-5.

[27] P. Jasik, J. Wilczyński, J.E. Sienkiewicz, Calculation of adiabatic potentials of Li_2^+, Eur. Phys. J. Spec. Top. 144 (1) (2007) 85–91, https://doi.org/10.1140/epjst/e2007-00111-2.

[28] P. Jasik, J. Sienkiewicz, Calculation of adiabatic potentials of Li_2, Chem. Phys. 323 (2) (2006) 563–573, https://doi.org/10.1016/j.chemphys.2005.10.025, http://www.sciencedirect.com/science/article/pii/S0301010405005380.

[29] R.J.L. Roy, Level: A computer program for solving the radial Schrödinger equation for bound and quasibound levels, Journal of Quantitative Spectroscopy and Radiative Transfer 186 (2017) 167 – 178, satellite Remote Sensing and Spectroscopy: Joint ACE-Odin Meeting, October 2015.https://doi.org/10.1016/j.jqsrt.2016.05.028,http://www.sciencedirect.com/science/article/pii/S0022407316300978.

[30] P. Fuentealba, H. Preuss, H. Stoll, L.V. Szentpály, A proper account of core-polarization with pseudopotentials: single valence-electron alkali compounds, Chem. Phys. Lett. 89 (5) (1982) 418–422, https://doi.org/10.1016/0009-2614(82)80012-2.

[31] B.P. Prascher, D.E. Woon, K.A. Peterson, T.H. Dunning, A.K. Wilson, Gaussian basis sets for use in correlated molecular calculations. VII. Valence, core-valence, and scalar relativistic basis sets for Li, Be, Na, and Mg, Theor. Chem. Acc. 128 (1) (2011) 69–82.https://doi.org/10.1007/s00214-010-0764-0.

[32] H. Silberbach, P. Schwerdtfeger, H. Stoll, H. Preuss, Ground and excited states of Rb_2^+ and Cs_2^+ by means of quasi-relativistic pseudo-potentials including core polarisation, J. Phys. B: At. Mol. Phys. 19 (5) (1986) 501,http://stacks.iop.org/0022-3700/19/i=5/a=011.

[33] L.V. Szentpály, P. Fuentealba, H. Preuss, H. Stoll, Pseudopotential calculations on Rb_2^+, Cs_2^+, RbH^+, CsH^+ and the mixed alkali dimer ions, Chem. Phys. Lett. 93 (6) (1982) 555 – 559,https://doi.org/10.1016/0009-2614(82)83728-7.

[34] P. Fuentealba, H. Stoll, L.V. Szentpály, P. Schwerdtfeger, H. Preuss, On the reliability of semi-empirical pseudopotentials: simulation of Hartree-Fock and Dirac-Fock results, J. Phys. B: At. Mol. Phys. 16 (11) (1983) L323, http://stacks.iop.org/0022-3700/16/i=11/a=00.

[35] I.S. Lim, P. Schwerdtfeger, B. Metz, H. Stoll, All-electron and relativistic pseudopotential studies for the group 1 element polarizabilities from K to element 119, J. Chem. Phys. 122 (10) (2005) 104103, https://doi.org/10.1063/1.1856451.

[36] E. Czuchaj, M. Krośnicki, H. Stoll, Quasirelativistic valence ab initio calculation of the potential-energy curves for Cd–rare gas atom pairs, Theoret. Chem. Acc. 105 (3) (2001) 219–226, https://doi.org/10.1007/s002140000206.

[37] S. Soorkia, F.L. Quéré, C. Lónard, D. Figgen, Ab initio study of the spinorbit coupling between the $A^1\Sigma_u^+$ and $b^3\Pi_u$ electronic states of Na_2, Mol. Phys. 105 (9) (2007) 1095–1104, https://doi.org/10.1080/00268970601161574.

[38] J.E. Sansonetti, Wavelengths, Transition Probabilities, and Energy Levels for the Spectra of Rubidium (Rb I through Rb XXXVII), J. Phys. Chem. Ref. Data 35 (1) (2006) 301–421, https://doi.org/10.1063/1.2035727, 10.1063/1.2035727.

[39] J.E. Sansonetti, Wavelengths, transition probabilities, and energy levels for the spectra of rubidium (Rb I through Rb XXXVII), J. Phys. Chem. Ref. Data 35 (1) (2006) 301–421, https://doi.org/10.1063/1.2035727.

[40] G. Herzberg, Molecular Spectra and Molecular Structure: Spectra of diatomic molecules, Molecular Spectra and Molecular Structure, R.E. Krieger Publishing Company, 1989.